Cell Reports

LFA1 and ICAM1 are critical for fusion and spread of murine leukemia virus *in vivo*

Graphical abstract

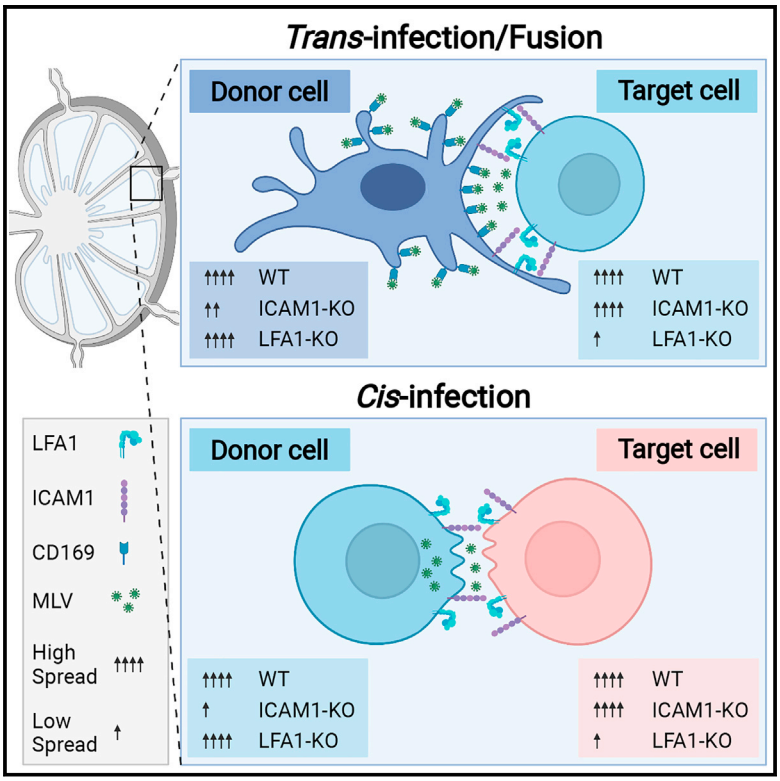

Highlights

- LFA1 and ICAM1 are important for cell-contact-dependent spread of MLV *in vivo*
- LFA1 on target cells is critical for MLV *cis*- and *trans*-infection
- ICAM1 on donor cells is critical for MLV *cis*-infection
- MLV fusion is not a limiting step to establish infection *in vivo*

Authors

Rebecca Engels, Lisa Falk, Manuel Albanese, Oliver T. Keppler, Xaver Sewald

Correspondence

sewald@mvp.lmu.de

In brief

Retroviruses can infect lymphocytes through direct cell-cell contacts. Engels et al. show that the retrovirus MLV requires the host cell adhesion protein LFA1 and its ligand ICAM1 for efficient spread *in vitro* and *in vivo*. The LFA1-ICAM1 interaction is important for cell-contact-dependent infection of lymphocyte subsets with MLV.

Engels et al., 2022, Cell Reports *38*, 110279
January 18, 2022
https://doi.org/10.1016/j.celrep.2021.110279

Cell Reports

CellPress
OPEN ACCESS

Report

LFA1 and ICAM1 are critical for fusion and spread of murine leukemia virus *in vivo*

Rebecca Engels,[1,3] Lisa Falk,[1,3] Manuel Albanese,[1,2] Oliver T. Keppler,[1] and Xaver Sewald[1,4,*]
[1]LMU München, Max von Pettenkofer Institute & Gene Center, Virology, National Reference Center for Retroviruses, Munich, Germany
[2]Present address: Istituto Nazionale Genetica Molecolare (INGM) 'Romeo ed Enrica Invernizzi', Milan, Italy
[3]These authors contributed equally
[4]Lead contact
*Correspondence: sewald@mvp.lmu.de
https://doi.org/10.1016/j.celrep.2021.110279

SUMMARY

Murine leukemia virus (MLV)-presenting cells form stable intercellular contacts with target cells during infection of lymphoid tissue, indicating a role of cell-cell contacts in retrovirus dissemination. Whether host cell adhesion proteins are required for retrovirus spread *in vivo* remains unknown. Here, we demonstrate that the lymphocyte-function-associated-antigen-1 (LFA1) and its ligand intercellular-adhesion-molecule-1 (ICAM1) are important for cell-contact-dependent transmission of MLV between leukocytes. Infection experiments in LFA1- and ICAM1-deficient mice demonstrate a defect in MLV spread within lymph nodes. Co-culture of primary leukocytes reveals a specific requirement for ICAM1 on donor cells and LFA1 on target cells for cell-contact-dependent spread through *trans*- and *cis*-infection. Importantly, adoptive transfer experiments combined with a newly established MLV-fusion assay confirm that the directed LFA1-ICAM1 interaction is important for retrovirus fusion and transmission *in vivo*. Taken together, our data provide insights on how retroviruses exploit host proteins and the biology of cell-cell interactions for dissemination.

INTRODUCTION

Retroviruses can spread efficiently between leukocytes across cell-cell contacts (Phillips, 1994; Sattentau, 2008). *In vitro* co-cultures of productively infected cells with non-infected target cells revealed contact-dependent transmission of HIV1, human T-lymphotropic virus type 1 (HTLV1), and murine leukemia virus (MLV) (*cis*-infection; Hubner et al., 2009; Igakura et al., 2003; Jin et al., 2009; Jolly et al., 2004; Sherer et al., 2007; Yamamoto et al., 1982). Thereby, retroviruses are transferred across a specialized cell-cell junction termed the virological synapse (VS) that is analogous to the immunological synapse (IS) (Vasiliver-Shamis et al., 2010). Further, transmission of surface-bound particles from non-infected cells across cell contacts supports retrovirus spread by a mechanism called *trans*-infection (Cameron et al., 1992; Geijtenbeek et al., 2000; McDonald et al., 2003). Lectin-binding proteins, such as CD169, on the surface of macrophages concentrate viral particles for *trans*-infection of target cells across infectious synapses (Erikson et al., 2015; Geijtenbeek et al., 2000; Hammonds et al., 2017; Izquierdo-Useros et al., 2012; Puryear et al., 2012; Sewald et al., 2015; Turville et al., 2002).

The integrin lymphocyte-function-associated-antigen-1 (LFA1) and its ligand intercellular-adhesion-molecule-1 (ICAM1) are critical factors of the immune response. Their function in lymphocyte migration and adhesion is crucial for processes such as immune cell priming (Dustin and Springer, 1989, 1991; Walling and Kim, 2018). Engagement of LFA1 with ICAM1 at intercellular contacts supports the formation of IS during T cell priming (Campi et al., 2005; Monks et al., 1998). A similar organization of cell-cell contacts was observed for VS formed between retrovirus-infected lymphocytes and non-infected T cells (Igakura et al., 2003; Jolly et al., 2004, 2007; Len et al., 2017; Starling and Jolly, 2016; Vasiliver-Shamis et al., 2008). Further, HIV-presenting dendritic cells (DCs) established infectious synapses with T cells during *trans*-infection with LFA1 accumulation at sites of cell-cell contact (McDonald et al., 2003). Antibody blocking revealed that the LFA1-ICAM1 interaction is important for cell-to-cell transmission of HIV by *trans*- and *cis*-infection *in vitro* (Arias et al., 2003; Jolly et al., 2007; Rodriguez-Plata et al., 2013; Sanders et al., 2002; Wang et al., 2009). The contribution of both proteins to retrovirus spread *in vivo* is currently unknown though.

Intravital microscopy at infected tissues revealed stable contacts between retrovirus-presenting and non-infected lymphocytes *in vivo* (Law et al., 2016; Murooka et al., 2012; Sewald et al., 2012, 2015). MLV-laden CD169^{+} macrophages at the popliteal lymph node (pLN) form Env-dependent cell-cell contacts with target cells preceding virus transfer for *trans*-infection (Sewald et al., 2015). Further, long-lasting contacts between retrovirus-infected lymphocytes and target cells were observed in MLV- and HIV-infected lymphoid tissues *in vivo* (Law et al., 2016; Murooka et al., 2012; Sewald et al., 2012, 2015). In addition to changes in cellular dynamics, the accumulation of the MLV capsid protein Gag at contact sites and the syncytia formation of HIV-infected cells indicate the existence of Env-dependent synaptic contacts *in vivo* (Law et al., 2016; Murooka et al., 2012; Sewald et al., 2012).

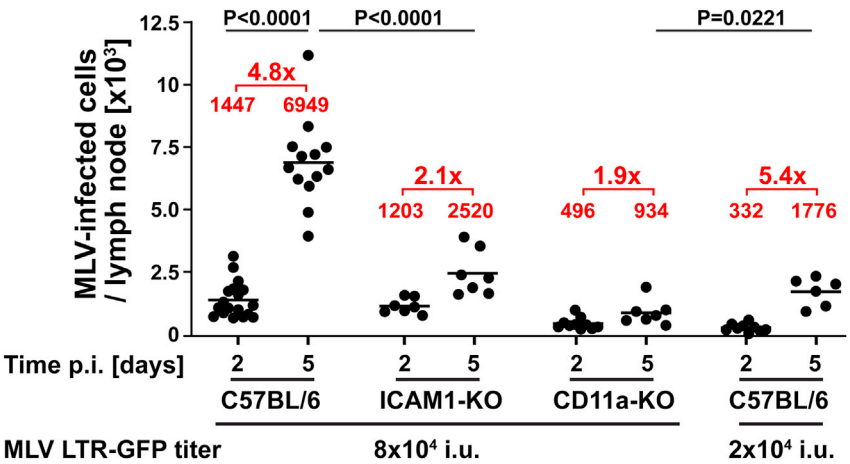

Figure 1. LFA1 and ICAM1 support local spread of MLV *in vivo*

Total MLV-infected cells in pLNs of C57BL/6, ICAM1-KO, and CD11a-KO mice 2 and 5 days post-injection (p.i.) of 8×10^4 infectious units (i.u.) (n = 13 for C57BL/6, n = 7 for ICAM1-KO, and n = 7 for CD11a-KO) and 2×10^4 i.u. (n = 6 for C57BL/6) of MLV LTR-GFP. Each point represents a pLN. Red numbers indicate mean number and fold changes (x-fold) of infected cells per pLN from 2 to 5 days p.i. See also Figure S1.

Although *in vivo* studies provide evidence for the formation of long-lasting cell-cell interactions during retroviral infection, a direct contribution of intercellular contacts to the spread of retroviruses *in vivo* remains elusive. Here, we investigate the role of the cell adhesion protein LFA1 and its ligand ICAM1 in retrovirus cell-to-cell transmission *in vivo*. Our data reveal that LFA1 and ICAM1 support MLV spread within lymphocyte populations of infected lymph nodes. We find that the specific interaction of LFA1 on target cells with ICAM1 on donor cells is critical for the efficient transmission of MLV by *trans*- and *cis*-infection. In addition, cell adhesion proteins were significant for fusion of MLV virions presented by $CD169^+$ macrophages at pLNs *in vivo*. Thus, our data demonstrate a critical role of host cell proteins in retrovirus spread, emphasizing the contribution of cell-cell contact to retrovirus transmission *in vivo*.

RESULTS

LFA1 and ICAM1 support retrovirus dissemination in lymph nodes

Retroviruses spread within lymphocyte populations of pLNs after subcutaneous (s.c.) virus delivery (Pi et al., 2019; Sewald et al., 2015; Uchil et al., 2019). To assess the contribution of cell-cell interactions to retrovirus spread *in vivo*, we used knockout (KO) mice deficient in the cell adhesion protein LFA1 (CD11a/CD18) and its ligand ICAM1 to follow MLV infection over time. Mice lacking the α subunit CD11a of the integrin LFA1 (CD11a-KO, LFA1 deficient), ICAM1-KO mice, and C57BL/6 wild-type (WT) mice were s.c. injected into the footpad with MLV long terminal repeat (LTR)-GFP. Infection at the draining pLNs was monitored at day 2 and 5 post-injection (p.i.) by quantification of GFP^+ cells (Figures 1 and S1A). MLV infection propagated in pLNs of C57BL/6 mice by ~5-fold within 3 days as the total number of GFP^+ cells increased from ~1,400 (mean value) at day 2 to ~7,000 at day 5 p.i. of 8×10^4 infectious units (i.u.). In contrast, the increase of MLV-infected cells in pLNs of mice lacking LFA1 and ICAM1 was reduced to ~2-fold. To exclude any bias caused by the lower initial infection rate in CD11a-KO mice at day 2 p.i., we infected C57BL/6 mice with a lower titer of MLV reporter virus (2×10^4 i.u.). Despite comparable levels of GFP^+ cells in pLNs of C57BL/6 mice and CD11a-KO mice at day 2, MLV spread was significantly higher in WT mice after 5 days of infection.

In summary, we observe a contribution of the integrin LFA1 and its ligand ICAM1 to the local dissemination of MLV in pLNs. The reduced spread of MLV in KO mice cannot be explained by differences in the cell tropism for T and B cell populations (Figures S1B and S1C).

LFA1 and ICAM1 support cell-contact-dependent spread of MLV *in vitro*

To confirm a role of cell adhesion in MLV spread, we developed *in vitro* co-culture assays with primary leukocytes (Figure S2A).

First, we characterized the MLV-infected lymphocyte populations in pLNs to use them as target cells in co-culture assays for *trans*- and *cis*-infection *ex vivo*. Previously, we identified B1 cells as the target cell type for MLV within the $CD19^+$ population (Pi et al., 2019; Sewald et al., 2015); the MLV-permissive $CD4^+$ T cell subset has remained unknown though. Surface marker analysis of MLV-infected $CD4^+$ T cells in pLNs of C57BL/6 mice revealed that MLV specifically targets T cells of the memory population (Figures 2A and S2B). More than 90% of infected $CD4^+$ T cells expressed the surface marker profile $CD62L^{low}$/$CD44^{high}$ and $CD62L^{high}$/$CD44^{high}$, representing effector memory T cells (T_{EM}) and central memory T cells (T_{CM}), respectively (Budd et al., 1987; Sallusto et al., 1999). Adoptive transfer of sorted RFP^+ $CD4^+$ T cell populations (T_{EM}, T_{CM}, and T_{NAIVE}) into C57BL/6 mice (Figure S2C) before s.c. infection with MLV confirmed T_{EM} and T_{CM} cells as specific MLV target cells in pLNs (Figures 2B and S2D). Similar to naive $CD19^+$ B cells (Sewald et al., 2015), MLV hardly infects the most abundant $CD4^+$ T cell population of naive cells ($CD62L^{high}$/$CD44^{low}$) early during infection (Figures 2A, 2B, and S2E). Interestingly, additional marker analysis revealed expression of FoxP3 in more than 60% of the infected memory cell population (Figures 2C and S2F). Therefore, we used *in vitro* differentiated $FoxP3^+$ $CD4^+$ T cells (Figure S2G) for subsequent assays.

Second, primary macrophages were isolated from the peritoneal cavity of mice (Figure S2H) to use them as donor cells for *trans*-infection. A thorough characterization revealed type I interferon (IFN)-supported surface expression of CD169 after ~24 h of *in vitro* culture (Figures 2D and S2I). CD169 was essential for retrovirus capture, because pre-treatment of macrophages with CD169-blocking antibodies significantly reduced MLV

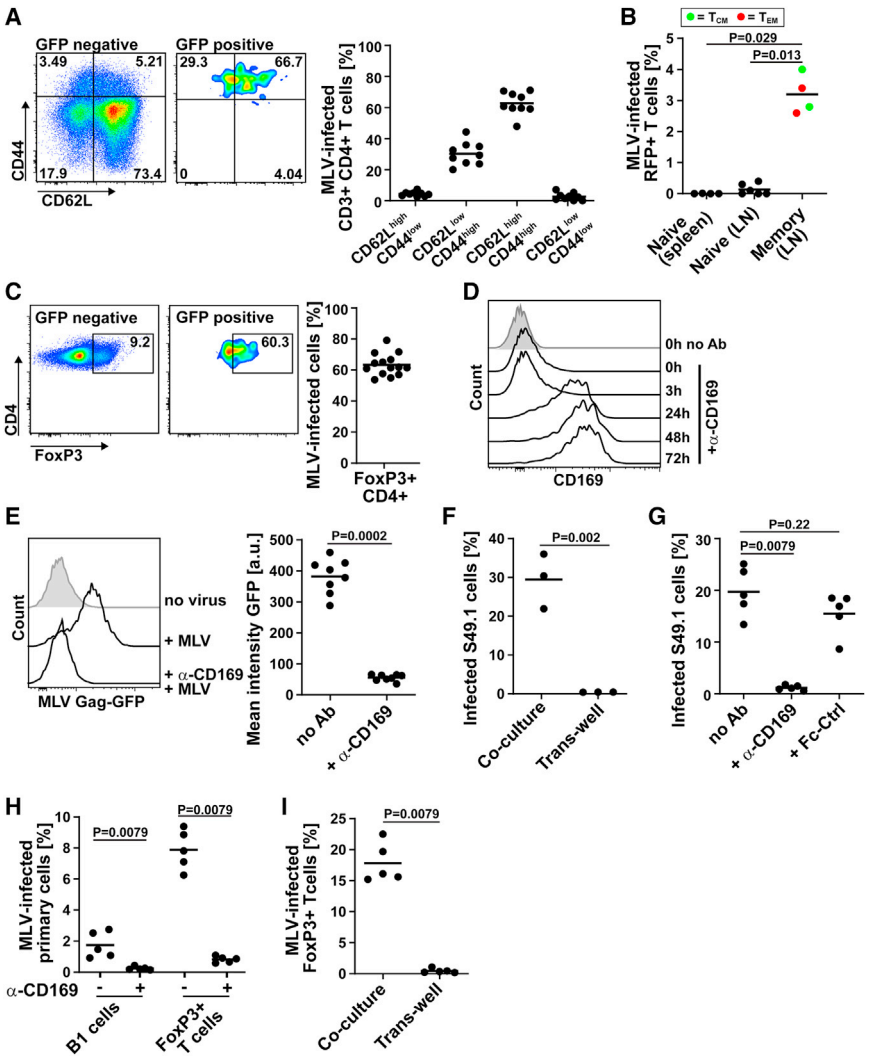

Figure 2. *In vitro* co-culture of primary cells supports cell-contact-dependent spread of MLV during *trans*- and *cis*-infection

(A) Analysis of MLV-infected (GFP-positive) and non-infected (GFP-negative) CD4$^+$ T cells characterized by CD62L and CD44 expression (n = 9).

(B) Infected, adoptively transferred RFP$^+$ naive T cells (spleen, n = 4; LNs, n = 6), central memory T cells (T_{CM}) (LNs, n = 2) and effector memory T cells (T_{EM}) (LNs, n = 2).

(C) Analysis of MLV-infected (GFP-positive) and non-infected (GFP-negative) CD4$^+$ T cells characterized by FoxP3 staining (n = 14).

(D) Surface CD169 expression by macrophages at different time points after *in vitro* cultivation (representative data from three independent experiments). Time points indicate hours of *in vitro* culture after cell isolation.

(E) CD169-dependent binding of MLV Gag-GFP (n = 8) to macrophages with or without CD169 blocking (n = 8).

(F and G) MLV-infected S49.1 cells after direct co-culture and culture in transwells with MLV-laden CD169$^+$ macrophages (F; n = 3) or with CD169$^+$ macrophages pre-treated with CD169 blocking or Fc control antibodies (G; n = 5).

(H) Infected target cells (B1 cells and FoxP3$^+$ T cells) after co-culture with MLV-laden CD169$^+$ macrophages (n = 5). Macrophages were pre-treated with antibodies against CD169 or left untreated.

(I) MLV-infected FoxP3$^+$ T cells after direct co-culture with MLV-infected B1 cells or separated cultivation in transwells (n = 5).

Cells were isolated from pLNs of C57BL/6 mice 2 days after subcutaneous (s.c.) MLV infection (A–C). See also Figure S2.

binding (Figure 2E). Importantly, *in vitro* cultured CD169$^+$ macrophages are not permissive to infection by virus-like particles (VLPs) pseudotyped with glycoproteins from ecotropic MLV or vesicular stomatitis virus (VSV) (Figure S2J) and therefore are suitable donor cells to study MLV *trans*-infection.

Finally, we tested the characterized primary cells to support cell-contact-dependent transmission of MLV *in vitro*. Co-culture experiments of MLV-laden CD169$^+$ macrophages (donor) with S49.1 T cells, primary B1 cells, or FoxP3$^+$ T cells (targets) separated by transwell inserts (Figures 2F and S2K) or in the presence of CD169-blocking antibodies (Figures 2G and 2H) confirm that *in vitro trans*-infection is cell contact dependent and requires CD169. *Cis*-infection assays of *in vitro* transduced B1 cells (donor) and FoxP3$^+$ T cells (target) reveal cell-contact-dependent MLV spread, because virus transmission to target cells was absent in cultures separated by transwell inserts (Figures 2I and S2L).

Next, the established co-culture assays were used to investigate the role of LFA1 and ICAM1 in *trans*- and *cis*-infection of MLV. We co-cultured MLV-laden CD169$^+$ macrophages (Figure S3A) or MLV-infected B1 cells (Figure S3B) with CD4$^+$ T cells in the presence of blocking antibodies against LFA1 or ICAM1. Quantification of GFP$^+$ CD4$^+$ T cells reveals a significant reduction in MLV-infected target cells after CD11a blocking compared with Fc control. Blocking of ICAM1 resulted in a minor reduction of infected cells during co-culture. In contrast, blocking of the alternative LFA1-ligand ICAM2, although highly expressed by relevant primary cells (Figure S3C), had no impact on *trans*-infection of target cells (Figure S3D). In summary, co-culture experiments with blocking antibodies indicate that LFA1 and ICAM1 contribute to cell-contact-dependent MLV transmission *in vitro*.

Unfortunately, blocking experiments do not allow addressing whether the orientation of receptor-ligand interaction is critical for MLV transmission, because primary cells used for co-cultures highly express both proteins (Figure S3C). To dissect the specific contribution of LFA1 and ICAM1 on donor and target cells individually, we performed co-cultures with combinations of WT and KO cells (Figures 3A–3D). Culturing of MLV-laden macrophages (*trans*-infection) or MLV-infected B1 cells (*cis*-infection) as donor cells together with FoxP3$^+$ T cells shows a major reduction in MLV-infected target cells lacking LFA1 (CD11a-KO; Figures 3A

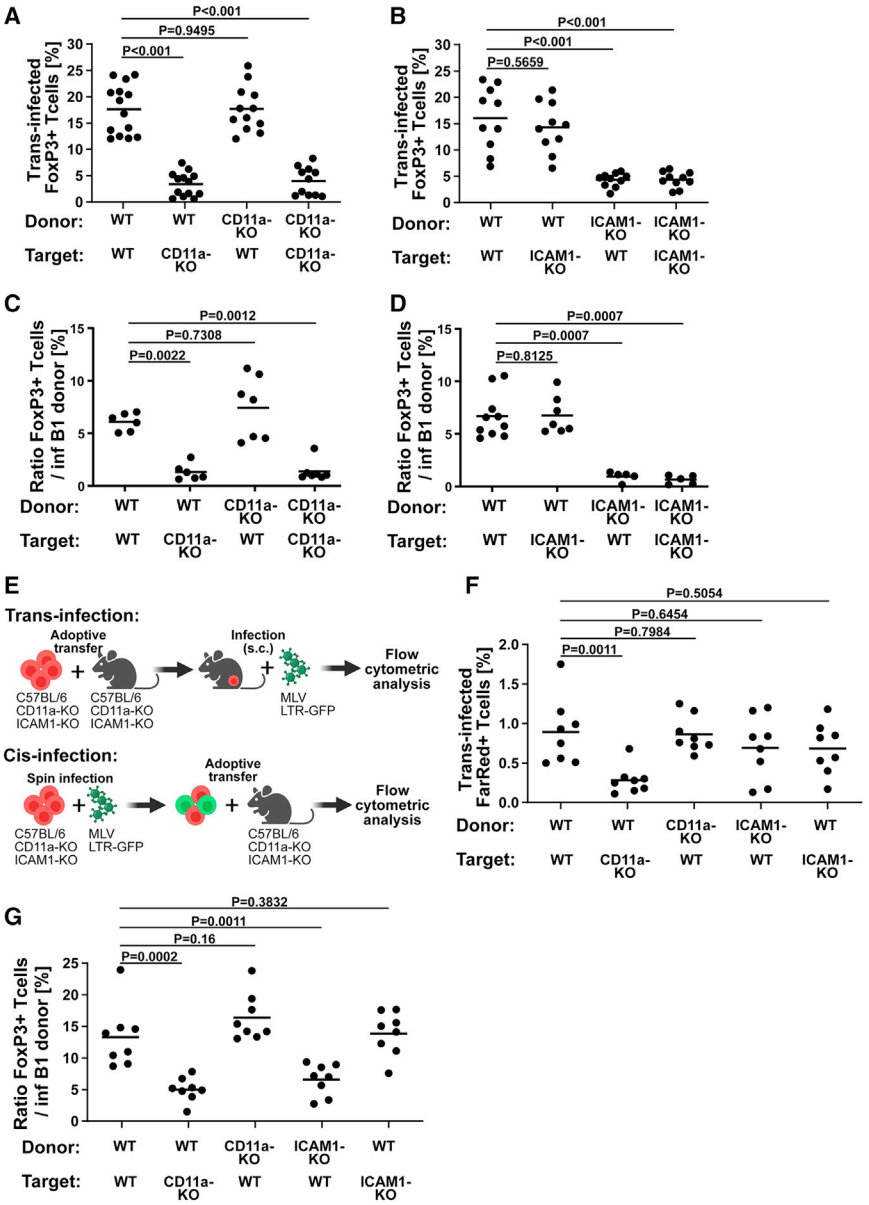

Figure 3. LFA1 and ICAM1 support cell-contact-dependent spread of MLV *in vitro* and *in vivo*

(A and B) Infected FoxP3$^+$ T cells (target) after co-culture with MLV-laden CD169$^+$ macrophages (donor) from WT C57BL/6, ICAM1-KO, and CD11a-KO mice. Co-cultures of cells from WT C57BL/6 and CD11a-KO mice (n = 10) are shown in (A), and WT C57BL/6 and ICAM1-KO mice (n = 10) are shown in (B).

(C and D) Infected FoxP3$^+$ T cells (target) after co-culture with MLV-infected B1 cells (donor) with cells from C57BL/6 and CD11a-KO mice (n = 6–7; C) and C57BL/6 and ICAM1-KO mice (n = 5–10; D). The ratio of infected target cells to MLV-infected donor B1 cells was used for quantification.

(E) Illustration of adoptive transfer experiments for *trans*- (upper panel) and *cis*-infection (lower panel) of MLV *in vivo*.

(F and G) Analysis of adoptive transfer experiments for *in vivo trans*- (F) and *cis*-infection (G) of MLV as described in (E). The percentage of MLV-infected cells (GFP$^+$ FarRed$^+$) of all adoptively transferred FarRed$^+$ T cells is used to quantify *trans*-infection rate (n = 8). The ratio of newly, *cis*-infected target cells (GFP$^+$ FarRed$^-$) relative to adoptively transferred MLV-infected donor cells (GFP$^+$ FarRed$^+$) is used to quantify *cis*-infection (n = 8).

See also Figure S3.

and 3C). Target cell infectivity is unchanged in co-cultures with LFA1-deficient donor cells compared with WT control (Figures 3A and 3C) or direct infection of target cells with cell-free MLV (Figure S3E). Importantly, ICAM1 is critical on the donor cell to support efficient *trans*- and *cis*-infection of MLV (Figures 3B and 3D). Transmission to target cells was reduced after co-culture with ICAM1-deficient donor cells despite similar MLV binding properties of WT and KO macrophages during *trans*-infection (Figure S3F).

In summary, co-culture assays reveal a specific requirement for ICAM1 on donor cells and LFA1 on target cells for efficient MLV spread between primary cells *in vitro*.

LFA1 and ICAM1 support spread of MLV *in vivo*

Infection of KO mice with MLV indicates a function of ICAM1 and LFA1 in retrovirus spread (Figure 1). However, the individual contribution of each protein on donor and target cells for *trans*- and *cis*-infection remains obscure *in vivo*. Therefore, adoptive transfer experiments with combinations of WT and KO cells transferred into WT and KO mice were conducted (Figure 3E). To address the role of LFA1 and ICAM1 in *trans*-infection, we injected fluorescently labeled (FarRed$^+$) FoxP3$^+$ T cells (WT, CD11a-KO, and ICAM1-KO) into C57BL/6, CD11a-KO, or ICAM1-KO mice before infection with MLV (Figure 3E, upper panel). Draining pLNs were analyzed, and the percentage of infected cells (GFP$^+$ FarRed$^+$) within the population of totally transferred cells (FarRed$^+$) was used for quantification (Figures 3F and S3G). Similar to *in vitro* co-cultures, LFA1 is required on target cells for efficient MLV *trans*-infection *in vivo*. Infection rates of LFA1-deficient FoxP3$^+$ T cells (target) in pLNs of WT C57BL/6 mice (donor) were reduced by 3-fold compared with WT target cells in CD11a-KO or C57BL/6 mice. Surprisingly, adoptive transfer of WT FoxP3$^+$ T cells into ICAM1-KO mice (donor) did not result in reduced infection of target cells. Differences in MLV capture at pLNs of WT and KO mice do not explain the results (Figure S3H).

To address the contribution of LFA1 and ICAM1 to retrovirus spread by *cis*-infection, FoxP3$^+$ T cells (WT, CD11a-KO, and ICAM1-KO) were transduced with MLV LTR-GFP and fluorescently labeled (FarRed$^+$) before adoptive transfer into WT and

KO mice (Figure 3E, lower panel). We analyzed pLNs for GFP$^+$ leukocytes and used the ratio of newly infected cells (GFP$^+$ FarRed$^-$) to MLV-infected donor cells (GFP$^+$ FarRed$^+$) to quantify adhesion-protein-dependent spread (Figures 3G and S3I). Excitingly, MLV spread from WT cells was significantly reduced after adoptive transfer into CD11a-KO mice, confirming a role of LFA1 on target cells for *cis*-infection *in vivo*, whereas LFA1 expression is negligible on donor cells (Figure 3G). Further, ICAM1 expression was required on donor cells to support efficient spread *in vivo*. MLV transmission from ICAM1-KO cells to WT cells in C57BL/6 mice was significantly reduced.

In summary, adoptive transfer experiments confirm a specific requirement for ICAM1 on infected donor cells and LFA1 on target cells for MLV spread by *cis*-infection *in vivo*. Although we can demonstrate a role of LFA1 on target cells for *trans*-infection, a contribution of ICAM1 was not obvious *in vivo*.

LFA1 supports fusion of MLV *in vivo*

Receptor binding and subsequent virus fusion with the host cell membrane are the first steps of the retroviral replication cycle ultimately leading to productive cell infection. Until now, we have shown that LFA1-ICAM1 interaction supports cell-contact-dependent infection with MLV (Figure 3).

To address whether both proteins also support retrovirus fusion *in vivo*, we established a novel assay using MLV CD63-BlaM LTR-GFP VLPs to quantify fusion and infection (Figure S4A). Incubation of permissive S49.1 cells with MLV VLPs pseudotyped with ecoEnv or VSV G protein (VSV-G) or lacking any glycoprotein (ΔEnv) resulted in more than 80% VLP-fused cells (ecoEnv and VSV-G) with almost no background signal (ΔEnv; Figure S4B). Because MLV VLPs contain the reporter genome LTR-GFP, CD63-BlaM LTR-GFP VLPs allowed us to monitor fusion and infection as shown for S49.1 cells (Figure S4C). Next, we used MLV VLPs to characterize the kinetics and cell tropism for MLV fusion *in vivo*. VLPs (ecoEnv and ΔEnv) were injected into C57BL/6 mice, and pLN cells were analyzed at different time points (Figure S4D). Fusion was first detectable 0.5 h p.i. and peaked (~3% of total cells) around 2 h p.i. (Figure 4A). In comparison, capture of fluorescent MLV Gag-GFP by CD169$^+$ macrophages culminates at 0.5–1 h p.i., preceding fusion with target cells by ~1 h (Figure 4A). Surface marker analysis of VLP-fused cells identified CD19$^+$ B cells and CD4$^+$ T cells (>90%) as the main cell types at different time points (Figures 4B and S4D–S4F). Within the CD4$^+$ T cell population, only ~30% of VLP-fused cells belong to the CD44$^+$ memory populations (including CD62L^{high} and CD62L^{low}) or expressed FoxP3 (Figures 4C, 4D, S4D, and S4E). Strikingly, the total number of fusion events at 2 h p.i. did not correlate with the total number of infected cells 48 h p.i. of single-round infectious VLPs (Figure 4E). Whereas ~9,000 VLP-fused cells were detected per pLN, only ~800 cells were productively infected as indicated by GFP expression. Excitingly, the total number of VLP-fused and -infected cells was almost identical in CD44^{high} and FoxP3$^+$ T cells (Figure 4F). In contrast, despite a high number of VLP-fused cells in the CD44^{low} population (naive and effector T cells), very few infected cells were detected (Figure 4F).

To address a role of LFA1 and ICAM1 in CD169$^+$ macrophages-mediated virion fusion with target cells *in vivo*, we applied adoptive transfer experiments similar to Figure 3E (upper panel). After adoptive transfer of FarRed$^+$ target cells into WT or KO mice (donor), fusion of VLPs with adoptively transferred cells was analyzed 2 h p.i. (Figures 4G and S4G). Whereas efficient fusion with VLPs required LFA1 expression of target cells, a contribution of ICAM1 on donor cells to VLP fusion *in vivo* was not obvious (Figure 4G).

In summary, the analysis of virion fusion *in vivo* reveals similar kinetic and cell specificity as described for MLV capture and *trans*-infection (Sewald et al., 2015). MLV VLP fusion was predominant within B and T cell populations but barely detectable for CD169$^+$ macrophages, cells that initially capture lymph-derived retroviruses. CD169$^+$ macrophage-mediated MLV *trans*-fusion required LFA1 on target lymphocytes, indicating a role of cell-cell interactions for specific fusion *in vivo*.

DISCUSSION

Stable cell-cell contacts were visualized in MLV- and HIV-infected lymphoid tissues, indicating that retrovirus-presenting cells locally spread the infection through VSs (Ladinsky et al., 2014; Law et al., 2016; Murooka et al., 2012; Sewald et al., 2012, 2015). Contacts were retrovirus induced and/or stabilized since they decreased after infection with mutant retroviruses lacking the Env glycoprotein or Env with reduced receptor-binding capacity (Law et al., 2016; Sewald et al., 2012, 2015). However, the functional link that the observed cell-cell contacts contribute to the spread of the infection is difficult because of the use of non-infectious retrovirus mutants. Here, we used a different approach by removing host cell adhesion proteins, known to mediate cell-cell contacts of leukocytes, in the context of WT retrovirus infection. Infection experiments in LFA1- and ICAM1-deficient mice (Figures 1 and 3) with WT MLV clearly demonstrate a role of cell adhesion in the local dissemination of MLV *in vivo*. MLV infection spread by a factor of 4.8 within 3 days, i.e., an estimated doubling time of 1.69 per day, in WT mice. In the absence of LFA1 or ICAM1, we observe a significant reduction in MLV spread (factor ~2) that corresponds to a doubling time of 1.24 and 1.28 per day, respectively. In summary, these data demonstrate that the cell adhesion proteins LFA1 and ICAM1 are critical host factors for the efficient spread of MLV *in vivo* and thereby support the concept that cell-cell contacts drive retrovirus infection. Modeling of retrovirus spread (Imle et al., 2019; Iwami et al., 2015; Zhang et al., 2015) further strengthens the relevance of cell-contact-dependent transmission.

LFA1 and ICAM1 are critical components of the immune system (Choudhuri et al., 2014; Dustin and Springer, 1989; Jenkins and Griffiths, 2010; Monks et al., 1998), and some of their intrinsic properties were described to be relevant for retrovirus infection *in vitro*. Initially observed to accumulate at contact sites of retrovirus-presenting leukocytes with non-infected target cells (Igakura et al., 2003; Jolly et al., 2004; McDonald et al., 2003), LFA1 and ICAM1 were shown to functionally contribute to retrovirus transmission *in vitro* (Arias et al., 2003; Jolly et al., 2007; Rodriguez-Plata et al., 2013; Sanders et al., 2002; Wang et al., 2009). Blocking antibodies prove a role of integrins in HIV spread, although contradicting results are reported (Puigdomenech et al., 2008). Alternative approaches using mutant cell lines lacking LFA1 or silencing of ICAM1 expression confirm their

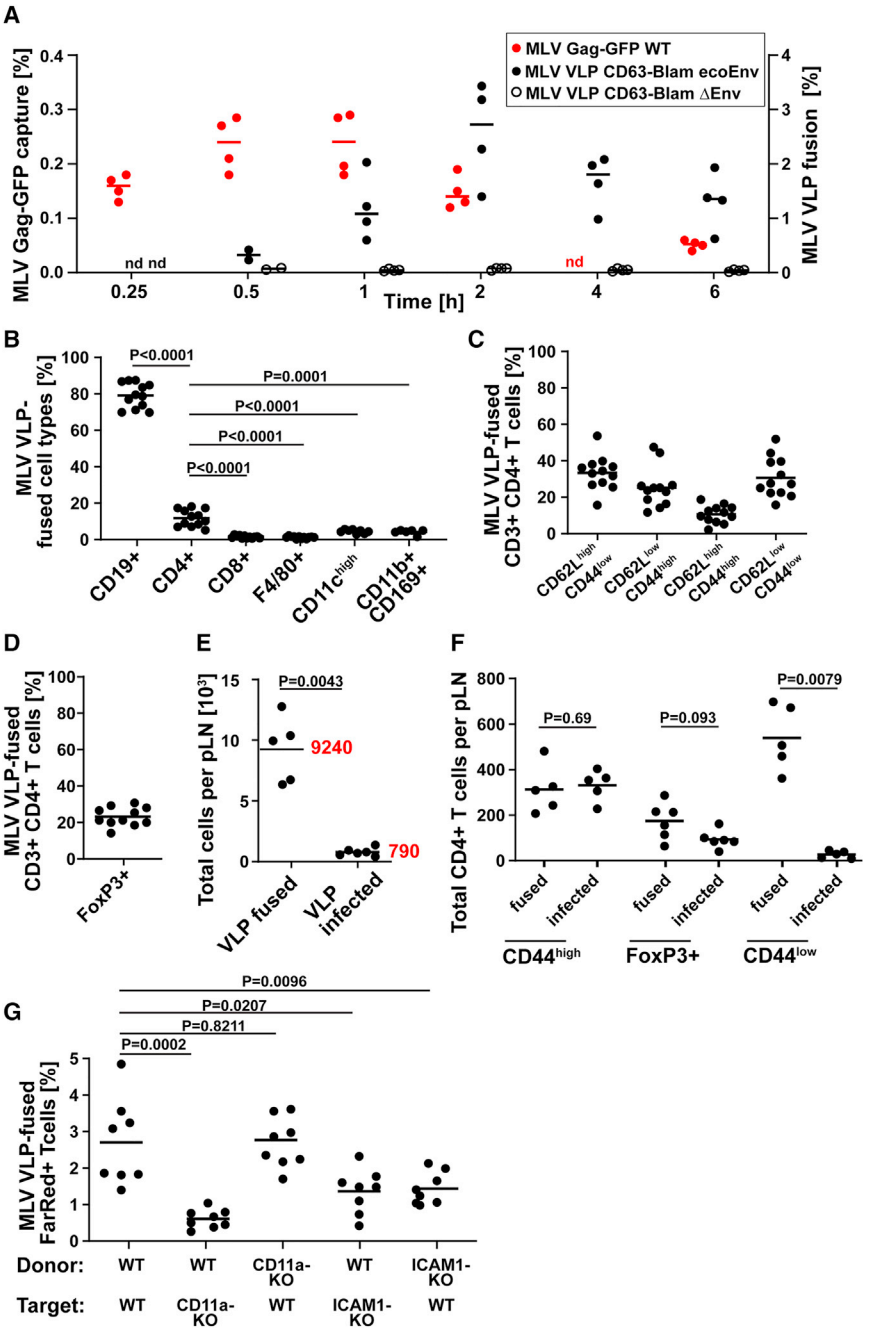

Figure 4. LFA1 expression on target lymphocytes supports fusion with MLV *in vivo*

(A) Capture of MLV Gag-GFP and fusion of MLV CD63-BlaM VLPs containing ecotropic MLV glycoprotein (ecoEnv) or lacking glycoprotein (ΔEnv) at different time points after s.c. injection. nd, not determined. n = 2–4.

(B–D) Analysis of VLP-fused cells at pLNs 2 h after MLV CD63-BlaM VLPs injection. Surface markers for leukocytes (B; n = 12) and CD4$^+$ T cells (C; n = 12) or staining of FoxP3 (D; n = 11) are used for characterization.

(E) Total number of pLN cells that fused with (2 h; n = 5) and were productively infected (48 h; n = 6) by MLV CD63-BlaM LTR-GFP VLPs.

(F) Total numbers of MLV VLP-fused (2 h) and -infected (48 h) CD4$^+$ T cell subsets (CD44^{high}, FoxP3$^+$, and CD44^{low}). Samples shown in (E) were analyzed for CD4$^+$ T cells after CD44 and FoxP3 staining. n = 5–6.

(G) Quantification of MLV VLPs fusion with adoptively transferred FoxP3$^+$ T cells. The percentage of fused FarRed$^+$ target cells (FarRed$^+$ and CCF4$_{cleaved}$) to transferred FarRed$^+$ FoxP3$^+$ T cells is shown (n = 8).

See also Figure S4.

contribution to cell-to-cell transmission of HIV (Hioe et al., 2001; Jolly et al., 2007; Wang et al., 2009). Further, *in vitro* co-cultures using primary cells from immunodeficient patients with nonfunctional LFA1 support a contribution of LFA1 to HIV transmission (Groot et al., 2006). The contribution of LFA1 and ICAM1 to HIV spread *in vivo* remains elusive though.

We have established *in vitro* co-cultures with relevant primary cell types to extend our knowledge of LFA1 and ICAM1 in cell-contact-dependent retrovirus spread. Using primary cells isolated from WT and KO mice, we could demonstrate that the polarity in the LFA1-ICAM1 interaction is relevant for MLV transmission. Whereas ICAM1 was critical on the MLV-presenting donor cells, LFA1 was important on the target cell during *trans*- and *cis*-infection.

We were further able to validate that both cell adhesion proteins significantly contribute to retrovirus spread *in vivo* (Figure S4H). Our model of retrovirus spread in lymphoid tissue confirmed that LFA1 on target cells is critical for MLV *trans*- and *cis*-infection of lymphocyte subsets. Retrovirus spread from MLV-infected FoxP3$^+$ T cells through *cis*-infection also required the expression of ICAM1 by donor cells, confirming the polarity in the LFA1-ICAM1 interaction. Interestingly, the expression of ICAM1 on donor macrophages was not essential during *trans*-infection at pLNs, indicating that other LFA1 ligands can contribute to MLV *trans*-infection *in vivo*. Although *in vitro* co-cultures with peritoneal-cavity-derived macrophages indicate that ICAM2 does not contribute to *trans*-infection of MLV, an alternative mechanism might compensate for the lack of ICAM1 *in vivo*. Lymph or serum proteins containing integrin-binding motifs might recognize MLV particles and function as bridging factors to mediate cell-cell contacts for *trans*-infection *in vivo*, as recently described for the glycoprotein MFG-E8 during retrovirus infection (Park and Kehrl, 2019).

The characterization of infected CD4$^+$ T cells revealed that MLV specifically targets memory T cells, T_{CM} and T_{EM}, as well

as FoxP3$^+$ T cells to establish infection *in vivo*. Previously, B1 cells were identified as a highly susceptible cell population in pLNs (Pi et al., 2019; Sewald et al., 2015). Targeting of B1 cells required sensing of incoming MLV since TLR7-deficient B1 cells were not susceptible to infection (Pi et al., 2019). Whether innate sensing of MLV is also essential for the initial infection of memory and FoxP3$^+$ T cells remains to be determined. During the course of an infection, MLV extends its cell tropism and infects naive cell populations, including naive B cells (Pi et al., 2019) and naive T cells (CD62L^{high}/CD44^{low}; Figure S2M). An activating environment within the infected tissue could favor the infection of naive lymphocytes and extend the pool of susceptible cells for MLV, as previously described for mouse mammary tumor virus (MMTV) (Kane et al., 2011; Wilks et al., 2015).

MLV requires the breakdown of the nuclear envelope during mitosis to integrate its proviral DNA into the host genome (Roe et al., 1993), emphasizing the role of cellular activation for MLV infection of lymphocytes. Therefore, adhesion-protein-mediated signaling might contribute to the susceptibility of target cells through activation-induced proliferation. LFA1 was shown to deliver a co-stimulatory signal after ICAM1 binding, supporting activation of resting CD4$^+$ T cells (Lebedeva et al., 2005; Van Seventer et al., 1990). In addition, viral proteins might support cellular activation and infection through interaction with cell adhesion proteins. HIV gp120 can deliver a co-stimulatory signal in CD4$^+$ T cells through interaction with the integrin $\alpha4\beta7$ (Goes et al., 2020). A phosphoproteomics analysis revealed that more than 200 host cell proteins are manipulated during HIV-1 spread (Len et al., 2017). Unfortunately, the contribution of adhesion molecules to the signaling could not be dissected.

Establishing infection within the host by targeting specific cell subsets within local tissues is considered a bottleneck for retroviruses *in vivo* (Haase, 2005). Thereby, the low frequency of MLV target cells at the time point of infection might be a limiting factor for the productive infection of cells. Alternatively, an additional bottleneck might exist at the level of retroviral particle fusion with target cells. Applying a BlaM-based VLP fusion assay *in vivo*, we were able to demonstrate that fusion is not the limiting step for MLV to establish infection in lymphoid tissue *in vivo*. Despite the high fusion rate of MLV with the CD44^{low} CD4$^+$ T cell population, including naive CD4$^+$ T cells, most cells are not permissive to MLV, possibly because of restriction factors that block infection before integration. Whether these cells, however, play a role in the immune response to MLV through innate sensing of the infection or indirectly support MLV spread by creating an activating tissue environment needs to be determined.

Limitations of the study

In this study, we demonstrate that the adhesion proteins ICAM1 and LFA1 support cell-contact-dependent spread of MLV in pLNs of infected mice, which may not reflect their contribution in other lymphoid or mucosal tissues during infection. Further, we provide evidence for a role of ICAM1 on donor cells and LFA1 on target cells for *cis*-infection *in vivo*. However, ICAM1 was not required on donor cells during *trans*-infection. Because of technical limitations, we were not able to identify the alternative LFA1 ligand expressed by macrophages at the subcapsular sinus (SCS) floor of pLNs. Further, whether macrophage populations of other infected tissues support *trans*-infection independently of ICAM1 remains to be determined.

STAR★METHODS

Detailed methods are provided in the online version of this paper and include the following:

- KEY RESOURCES TABLE
- RESOURCE AVAILABILITY
  - Lead contact
  - Materials availability
  - Data and code availability
- EXPERIMENTAL MODEL AND SUBJECT DETAILS
  - Mice
  - Cell lines and primary cell cultures
- METHOD DETAILS
  - Primary cell isolation
  - Primary cell activation and differentiation *in vitro*
  - Virus preparation
  - *In vitro trans*-infection assay
  - *In vitro* transduction of primary cells with MLV
  - *In vitro cis*-infection assay
  - CD169 expression by primary macrophages
  - MLV Gag-GFP binding by CD169 + macrophages
  - *In vitro* transduction of macrophages with MLV VLPs
  - Retrovirus capture and infection *in vivo*
  - Flow cytometry
  - Adoptive transfer experiments
  - *In vivo cis*-infection assay
  - *In vivo trans*-infection and fusion assay
  - *In vitro* and *in vivo* fusion assay
- QUANTIFICATION AND STATISTICAL ANALYSIS

SUPPLEMENTAL INFORMATION

Supplemental information can be found online at https://doi.org/10.1016/j.celrep.2021.110279.

ACKNOWLEDGMENTS

This work was supported by DFG grant SE 2724/1-1 to X.S. We thank Nasim Motamedi and Avinash Shenoy for suggestions. Schematic illustrations were created with BioRender.com.

AUTHOR CONTRIBUTIONS

Conceptualization and methodology, R.E., L.F., and X.S.; investigation, R.E., L.F., and X.S.; visualization, X.S.; writing – original draft, R.E., L.F., and X.S.; writing – review & editing, M.A. and O.T.K.; resources, M.A.; funding acquisition, X.S.

DECLARATION OF INTERESTS

The authors declare no competing interests.

Received: June 7, 2021
Revised: October 18, 2021
Accepted: December 23, 2021
Published: January 18, 2022

SUPPORTING CITATIONS

The following references appear in the supplemental information: Cavrois et al. (2002); Segura et al. (2008); Sherer et al. (2003).

REFERENCES

Albanese, M., Chen, Y.-F.A., Hüls, C., Gärtner, K., Tagawa, T., Mejias-Perez, E., Keppler, O.T., Göbel, C., Zeidler, R., Shein, M., et al. (2020). Micro RNAs are minor constituents of extracellular vesicles and are hardly delivered to target cells. PLoS Genet. *17*, e1009951. https://doi.org/10.1101/2020.05.20.106393.

Arias, R.A., Munoz, L.D., and Munoz-Fernandez, M.A. (2003). Transmission of HIV-1 infection between trophoblast placental cells and T-cells take place via an LFA-1-mediated cell to cell contact. Virology *307*, 266–277. https://doi.org/10.1016/s0042-6822(02)00040-5.

Budd, R.C., Cerottini, J.C., Horvath, C., Bron, C., Pedrazzini, T., Howe, R.C., and MacDonald, H.R. (1987). Distinction of virgin and memory T lymphocytes. Stable acquisition of the Pgp-1 glycoprotein concomitant with antigenic stimulation. J. Immunol. *138*, 3120–3129.

Cameron, P.U., Freudenthal, P.S., Barker, J.M., Gezelter, S., Inaba, K., and Steinman, R.M. (1992). Dendritic cells exposed to human immunodeficiency virus type-1 transmit a vigorous cytopathic infection to CD4+ T cells. Science *257*, 383–387.

Campi, G., Varma, R., and Dustin, M.L. (2005). Actin and agonist MHC-peptide complex-dependent T cell receptor microclusters as scaffolds for signaling. J. Exp. Med. *202*, 1031–1036. https://doi.org/10.1084/jem.20051182.

Cavrois, M., De Noronha, C., and Greene, W.C. (2002). A sensitive and specific enzyme-based assay detecting HIV-1 virion fusion in primary T lymphocytes. Nat. Biotechnol. *20*, 1151–1154.

Choudhuri, K., Llodra, J., Roth, E.W., Tsai, J., Gordo, S., Wucherpfennig, K.W., Kam, L.C., Stokes, D.L., and Dustin, M.L. (2014). Polarized release of T-cell-receptor-enriched microvesicles at the immunological synapse. Nature *507*, 118–123. https://doi.org/10.1038/nature12951.

Dustin, M.L., and Springer, T.A. (1989). T-cell receptor cross-linking transiently stimulates adhesiveness through LFA-1. Nature *341*, 619–624. https://doi.org/10.1038/341619a0.

Dustin, M.L., and Springer, T.A. (1991). Role of lymphocyte adhesion receptors in transient interactions and cell locomotion. Annu. Rev. Immunol. *9*, 27–66. https://doi.org/10.1146/annurev.iy.09.040191.000331.

Erikson, E., Wratil, P.R., Frank, M., Ambiel, I., Pahnke, K., Pino, M., Azadi, P., Izquierdo-Useros, N., Martinez-Picado, J., Meier, C., et al. (2015). Mouse siglec-1 mediates trans-infection of surface-bound murine leukemia virus in a sialic acid N-acyl side chain-dependent manner. J. Biol. Chem. *290*, 27345–27359. https://doi.org/10.1074/jbc.M115.681338.

Geijtenbeek, T.B., Kwon, D.S., Torensma, R., van Vliet, S.J., van Duijnhoven, G.C., Middel, J., Cornelissen, I.L., Nottet, H.S., KewalRamani, V.N., Littman, D.R., et al. (2000). DC-SIGN, a dendritic cell-specific HIV-1-binding protein that enhances trans-infection of T cells. Cell *100*, 587–597.

Goes, L.R., Sajani, A., Sivro, A., Olowojesiku, R., Ray, J.C., Perrone, I., Yolitz, J., Girard, A., Leyre, L., Wibmer, C.K., et al. (2020). The V2 loop of HIV gp120 delivers costimulatory signals to CD4(+) T cells through Integrin alpha4beta7 and promotes cellular activation and infection. Proc. Natl. Acad. Sci. U S A *117*, 32566–32573. https://doi.org/10.1073/pnas.2011501117.

Groot, F., Kuijpers, T.W., Berkhout, B., and de Jong, E.C. (2006). Dendritic cell-mediated HIV-1 transmission to T cells of LAD-1 patients is impaired due to the defect in LFA-1. Retrovirology *3*, 75. https://doi.org/10.1186/1742-4690-3-75.

Haase, A.T. (2005). Perils at mucosal front lines for HIV and SIV and their hosts. Nat. Rev. Immunol. *5*, 783–792. https://doi.org/10.1038/nri1705.

Hammonds, J.E., Beeman, N., Ding, L., Takushi, S., Francis, A.C., Wang, J.J., Melikyan, G.B., and Spearman, P. (2017). Siglec-1 initiates formation of the virus-containing compartment and enhances macrophage-to-T cell transmission of HIV-1. PLoS Pathog. *13*, e1006181. https://doi.org/10.1371/journal.ppat.1006181.

Hioe, C.E., Chien, P.C., Jr., Lu, C., Springer, T.A., Wang, X.H., Bandres, J., and Tuen, M. (2001). LFA-1 expression on target cells promotes human immunodeficiency virus type 1 infection and transmission. J. Virol. *75*, 1077–1082. https://doi.org/10.1128/JVI.75.2.1077-1082.2001.

Hubner, W., McNerney, G.P., Chen, P., Dale, B.M., Gordon, R.E., Chuang, F.Y., Li, X.D., Asmuth, D.M., Huser, T., and Chen, B.K. (2009). Quantitative 3D video microscopy of HIV transfer across T cell virological synapses. Science *323*, 1743–1747. https://doi.org/10.1126/science.1167525.

Igakura, T., Stinchcombe, J.C., Goon, P.K., Taylor, G.P., Weber, J.N., Griffiths, G.M., Tanaka, Y., Osame, M., and Bangham, C.R. (2003). Spread of HTLV-I between lymphocytes by virus-induced polarization of the cytoskeleton. Science *299*, 1713–1716. https://doi.org/10.1126/science.1080115.

Imle, A., Kumberger, P., Schnellbacher, N.D., Fehr, J., Carrillo-Bustamante, P., Ales, J., Schmidt, P., Ritter, C., Godinez, W.J., Muller, B., et al. (2019). Experimental and computational analyses reveal that environmental restrictions shape HIV-1 spread in 3D cultures. Nat. Commun. *10*, 2144. https://doi.org/10.1038/s41467-019-09879-3.

Iwami, S., Takeuchi, J.S., Nakaoka, S., Mammano, F., Clavel, F., Inaba, H., Kobayashi, T., Misawa, N., Aihara, K., Koyanagi, Y., et al. (2015). Cell-to-cell infection by HIV contributes over half of virus infection. eLife *4*, e08150. https://doi.org/10.7554/eLife.08150.

Izquierdo-Useros, N., Lorizate, M., Contreras, F.X., Rodriguez-Plata, M.T., Glass, B., Erkizia, I., Prado, J.G., Casas, J., Fabrias, G., Krausslich, H.G., et al. (2012). Sialyllactose in viral membrane gangliosides is a novel molecular recognition pattern for mature dendritic cell capture of HIV-1. PLoS Biol. *10*, e1001315. https://doi.org/10.1371/journal.pbio.1001315.

Jenkins, M.R., and Griffiths, G.M. (2010). The synapse and cytolytic machinery of cytotoxic T cells. Curr. Opin. Immunol. *22*, 308–313. https://doi.org/10.1016/j.coi.2010.02.008.

Jin, J., Sherer, N.M., Heidecker, G., Derse, D., and Mothes, W. (2009). Assembly of the murine leukemia virus is directed towards sites of cell-cell contact. PLoS Biol. *7*, e1000163. https://doi.org/10.1371/journal.pbio.1000163.

Jolly, C., Kashefi, K., Hollinshead, M., and Sattentau, Q.J. (2004). HIV-1 cell to cell transfer across an Env-induced, actin-dependent synapse. J. Exp. Med. *199*, 283–293. https://doi.org/10.1084/jem.20030648.

Jolly, C., Mitar, I., and Sattentau, Q.J. (2007). Adhesion molecule interactions facilitate human immunodeficiency virus type 1-induced virological synapse formation between T cells. J. Virol. *81*, 13916–13921. https://doi.org/10.1128/JVI.01585-07.

Kane, M., Case, L.K., Kopaskie, K., Kozlova, A., MacDearmid, C., Chervonsky, A.V., and Golovkina, T.V. (2011). Successful transmission of a retrovirus depends on the commensal microbiota. Science *334*, 245–249. https://doi.org/10.1126/science.1210718.

Ladinsky, M.S., Kieffer, C., Olson, G., Deruaz, M., Vrbanac, V., Tager, A.M., Kwon, D.S., and Bjorkman, P.J. (2014). Electron tomography of HIV-1 infection in gut-associated lymphoid tissue. PLoS Pathog. *10*, e1003899. https://doi.org/10.1371/journal.ppat.1003899.

Law, K.M., Komarova, N.L., Yewdall, A.W., Lee, R.K., Herrera, O.L., Wodarz, D., and Chen, B.K. (2016). In vivo HIV-1 cell-to-cell transmission promotes multicopy micro-compartmentalized infection. Cell Rep. *15*, 2771–2783. https://doi.org/10.1016/j.celrep.2016.05.059.

Lebedeva, T., Dustin, M.L., and Sykulev, Y. (2005). ICAM-1 co-stimulates target cells to facilitate antigen presentation. Curr. Opin. Immunol. *17*, 251–258. https://doi.org/10.1016/j.coi.2005.04.008.

Len, A.C.L., Starling, S., Shivkumar, M., and Jolly, C. (2017). HIV-1 activates T cell signaling independently of antigen to drive viral spread. Cell Rep. *18*, 1062–1074. https://doi.org/10.1016/j.celrep.2016.12.057.

McDonald, D., Wu, L., Bohks, S.M., KewalRamani, V.N., Unutmaz, D., and Hope, T.J. (2003). Recruitment of HIV and its receptors to dendritic cell-T cell junctions. Science *300*, 1295–1297. https://doi.org/10.1126/science.1084238.

Monks, C.R., Freiberg, B.A., Kupfer, H., Sciaky, N., and Kupfer, A. (1998). Three-dimensional segregation of supramolecular activation clusters in T cells. Nature *395*, 82–86. https://doi.org/10.1038/25764.

Murooka, T.T., Deruaz, M., Marangoni, F., Vrbanac, V.D., Seung, E., von Andrian, U.H., Tager, A.M., Luster, A.D., and Mempel, T.R. (2012). HIV-infected T cells are migratory vehicles for viral dissemination. Nature *490*, 283–287. https://doi.org/10.1038/nature11398.

Park, C., and Kehrl, J.H. (2019). An integrin/MFG-E8 shuttle loads HIV-1 viral-like particles onto follicular dendritic cells in mouse lymph node. eLife *8*. https://doi.org/10.7554/eLife.47776.

Phillips, D.M. (1994). The role of cell-to-cell transmission in HIV infection. AIDS *8*, 719–731.

Pi, R., Iwasaki, A., Sewald, X., Mothes, W., and Uchil, P.D. (2019). Murine leukemia virus exploits innate sensing by toll-like receptor 7 in B-1 cells to establish infection and locally spread in mice. J. Virol. *93*. https://doi.org/10.1128/JVI.00930-19.

Puigdomenech, I., Massanella, M., Izquierdo-Useros, N., Ruiz-Hernandez, R., Curriu, M., Bofill, M., Martinez-Picado, J., Juan, M., Clotet, B., and Blanco, J. (2008). HIV transfer between CD4 T cells does not require LFA-1 binding to ICAM-1 and is governed by the interaction of HIV envelope glycoprotein with CD4. Retrovirology *5*, 32. https://doi.org/10.1186/1742-4690-5-32.

Puryear, W.B., Yu, X., Ramirez, N.P., Reinhard, B.M., and Gummuluru, S. (2012). HIV-1 incorporation of host-cell-derived glycosphingolipid GM3 allows for capture by mature dendritic cells. Proc. Natl. Acad. Sci. U S A *109*, 7475–7480. https://doi.org/10.1073/pnas.1201104109.

Rodriguez-Plata, M.T., Puigdomenech, I., Izquierdo-Useros, N., Puertas, M.C., Carrillo, J., Erkizia, I., Clotet, B., Blanco, J., and Martinez-Picado, J. (2013). The infectious synapse formed between mature dendritic cells and CD4(+) T cells is independent of the presence of the HIV-1 envelope glycoprotein. Retrovirology *10*, 42. https://doi.org/10.1186/1742-4690-10-42.

Roe, T., Reynolds, T.C., Yu, G., and Brown, P.O. (1993). Integration of murine leukemia virus DNA depends on mitosis. EMBO J. *12*, 2099–2108.

Sallusto, F., Lenig, D., Forster, R., Lipp, M., and Lanzavecchia, A. (1999). Two subsets of memory T lymphocytes with distinct homing potentials and effector functions. Nature *401*, 708–712. https://doi.org/10.1038/44385.

Sanders, R.W., de Jong, E.C., Baldwin, C.E., Schuitemaker, J.H., Kapsenberg, M.L., and Berkhout, B. (2002). Differential transmission of human immunodeficiency virus type 1 by distinct subsets of effector dendritic cells. J. Virol. *76*, 7812–7821. https://doi.org/10.1128/jvi.76.15.7812-7821.2002.

Sattentau, Q. (2008). Avoiding the void: cell-to-cell spread of human viruses. Nat. Rev. Microbiol. *6*, 815–826. https://doi.org/10.1038/nrmicro1972.

Segura, M.M., Garnier, A., Di Falco, M.R., Whissell, G., Meneses-Acosta, A., Arcand, N., and Kamen, A. (2008). Identification of host proteins associated with retroviral vector particles by proteomic analysis of highly purified vector preparations. J. Virol. *82*, 1107–1117.

Sewald, X., Gonzalez, D.G., Haberman, A.M., and Mothes, W. (2012). In Vivo imaging of virological synapses. Nat. Commun. *3*, 1320. https://doi.org/10.1038/ncomms2338.

Sewald, X., Ladinsky, M.S., Uchil, P.D., Beloor, J., Pi, R., Herrmann, C., Motamedi, N., Murooka, T.T., Brehm, M.A., Greiner, D.L., et al. (2015). Retroviruses use CD169-mediated trans-infection of permissive lymphocytes to establish infection. Science *350*, 563–567. https://doi.org/10.1126/science.aab2749.

Sherer, N.M., Lehmann, M.J., Jimenez-Soto, L.F., Ingmundson, A., Horner, S.M., Cicchetti, G., Allen, P.G., Pypaert, M., Cunningham, J.M., and Mothes, W. (2003). Visualization of retroviral replication in living cells reveals budding into multivesicular bodies. Traffic *4*, 785–801.

Sherer, N.M., Lehmann, M.J., Jimenez-Soto, L.F., Horensavitz, C., Pypaert, M., and Mothes, W. (2007). Retroviruses can establish filopodial bridges for efficient cell-to-cell transmission. Nat. Cell Biol. *9*, 310–315. https://doi.org/10.1038/ncb1544.

Starling, S., and Jolly, C. (2016). LFA-1 engagement triggers T cell polarization at the HIV-1 virological synapse. J. Virol. *90*, 9841–9854. https://doi.org/10.1128/JVI.01152-16.

Turville, S.G., Cameron, P.U., Handley, A., Lin, G., Pohlmann, S., Doms, R.W., and Cunningham, A.L. (2002). Diversity of receptors binding HIV on dendritic cell subsets. Nat. Immunol. *3*, 975–983. https://doi.org/10.1038/ni841.

Uchil, P.D., Pi, R., Haugh, K.A., Ladinsky, M.S., Ventura, J.D., Barrett, B.S., Santiago, M.L., Bjorkman, P.J., Kassiotis, G., Sewald, X., et al. (2019). A protective role for the lectin CD169/Siglec-1 against a pathogenic murine retrovirus. Cell Host Microbe *25*, 87–100 e110. https://doi.org/10.1016/j.chom.2018.11.011.

Van Seventer, G.A., Shimizu, Y., Horgan, K.J., and Shaw, S. (1990). The LFA-1 ligand ICAM-1 provides an important costimulatory signal for T cell receptor-mediated activation of resting T cells. J. Immunol. *144*, 4579–4586.

Vasiliver-Shamis, G., Dustin, M.L., and Hioe, C.E. (2010). HIV-1 virological synapse is not simply a copycat of the immunological synapse. Viruses *2*, 1239–1260. https://doi.org/10.3390/v2051239.

Vasiliver-Shamis, G., Tuen, M., Wu, T.W., Starr, T., Cameron, T.O., Thomson, R., Kaur, G., Liu, J., Visciano, M.L., Li, H., et al. (2008). Human immunodeficiency virus type 1 envelope gp120 induces a stop signal and virological synapse formation in noninfected CD4+ T cells. J. Virol. *82*, 9445–9457. https://doi.org/10.1128/JVI.00835-08.

Walling, B.L., and Kim, M. (2018). LFA-1 in T cell migration and differentiation. Front. Immunol. *9*, 952. https://doi.org/10.3389/fimmu.2018.00952.

Wang, J.H., Kwas, C., and Wu, L. (2009). Intercellular adhesion molecule 1 (ICAM-1), but not ICAM-2 and -3, is important for dendritic cell-mediated human immunodeficiency virus type 1 transmission. J. Virol. *83*, 4195–4204. https://doi.org/10.1128/JVI.00006-09.

Wilks, J., Lien, E., Jacobson, A.N., Fischbach, M.A., Qureshi, N., Chervonsky, A.V., and Golovkina, T.V. (2015). Mammalian lipopolysaccharide receptors incorporated into the retroviral envelope augment virus transmission. Cell Host Microbe *18*, 456–462. https://doi.org/10.1016/j.chom.2015.09.005.

Yamamoto, N., Okada, M., Koyanagi, Y., Kannagi, M., and Hinuma, Y. (1982). Transformation of human leukocytes by cocultivation with an adult T cell leukemia virus producer cell line. Science *217*, 737–739. https://doi.org/10.1126/science.6980467.

Zhang, C., Zhou, S., Groppelli, E., Pellegrino, P., Williams, I., Borrow, P., Chain, B.M., and Jolly, C. (2015). Hybrid spreading mechanisms and T cell activation shape the dynamics of HIV-1 infection. PLoS Comput. Biol. *11*, e1004179. https://doi.org/10.1371/journal.pcbi.1004179.

STAR★METHODS

KEY RESOURCES TABLE

REAGENT or RESOURCE	SOURCE	IDENTIFIER
Antibodies		
Ultra-LEAF purified anti-mouse CD169 (3D6.112)	Biolegend	Cat # 142,402
Ultra-LEAF purified Rat IgG2a isotype control antibody (RTK2758)	Biolegend	Cat # 400,516
Fc block anti mouse-CD16/CD32 (clone 93)	Biolegend	Cat # 101,302
CD169-PE (clone 3D6.112)	Biolegend	Cat # 142,403
CD169-AF647 (clone 3D6.112)	Biolegend	Cat # 142,407
CD11b-APC (clone M1/70)	Biolegend	Cat # 101,211
CD11b-BV421 (clone M1/70)	Biolegend	Cat # 101,251
CD11b-PE/Cy7 (clone M1/70)	Biolegend	Cat # 101,215
CD11a-APC (clone M17/4)	Biolegend	Cat # 101,119
CD11c-APC (clone N418)	Biolegend	Cat # 117,309
CD54-APC (clone YN1/1.7.4)	Biolegend	Cat # 116,119
CD3e-BV421 (clone 145-2C11)	Biolegend	Cat # 100,341
CD3-PE (clone 17A2)	Biolegend	Cat # 100,205
CD3e-PE/Cy7 (clone 145-2C11)	Biolegend	Cat # 100,319
CD4-APC/Fire750 (clone GK1.5)	Biolegend	Cat # 100,459
CD19-PE (clone 6D5)	Biolegend	Cat # 115,507
CD19-APC (clone 6D5)	Biolegend	Cat # 115,511
CD19-BV421 (clone 6D5)	Biolegend	Cat # 115,549
CD44-APC (clone IM7)	Biolegend	Cat # 103,011
CD44-BV605 (clone IM7)	Biolegend	Cat # 103,047
CD62L-BV421 (clone MEL-14)	Biolegend	Cat # 104,436
CD62L-PE/Cy7 (clone MEL-14)	Biolegend	Cat # 104,417
CD102-AF647 (clone 3C4[mIC2/4])	Biolegend	Cat # 105,611
FoxP3-AF647 (clone MF-14)	Biolegend	Cat # 126,408
FoxP3-PE (clone MF-14)	Biolegend	Cat # 126,403
F4/80-PE/Cy7 (clone BM8)	Biolegend	Cat # 123,113
Biotin anti-mouse CD19 Antibody	Biolegend	Cat # 115,503
Biotin anti-mouse CD8a Antibody	Biolegend	Cat # 100,704
Biotin anti-mouse CD4 Antibody	Biolegend	Cat # 100,507
Biotin anti-mouse Ly-6G/Ly-6C (Gr-1) Antibody	Biolegend	Cat # 108,403
Biotin anti-mouse TER-119/Erythroid Cells Antibody	Biolegend	Cat # 116,204
Biotin anti-mouse CD11c Antibody	Biolegend	Cat # 117,303
Biotin anti-mouse F4/80 Antibody	Biolegend	Cat # 123,106
Biotin anti-mouse CD8a Antibody	Biolegend	Cat # 100,704
Biotin anti-mouse CD4 Antibody	Biolegend	Cat # 100,507
Biotin anti-mouse Ly-6G/Ly-6C (Gr-1) Antibody	Biolegend	Cat # 108,403
Biotin anti-mouse TER-119/Erythroid Cells Antibody	Biolegend	Cat # 116,204
Biotin anti-mouse CD11c Antibody	Biolegend	Cat # 117,303
Biotin anti-mouse NK-1.1 Antibody	Biolegend	Cat # 108,704
Biotin anti-mouse CD23 Antibody	Biolegend	Cat # 101,603
Biotin anti-mouse FcεRIα Antibody	Biolegend	Cat # 134,304
Biotin anti-mouse CD88 (C5aR) Antibody	Biolegend	Cat # 135,811
Biotin anti-mouse CD117 (c-Kit) Antibody	Biolegend	Cat # 105,804

(*Continued on next page*)

Continued

REAGENT or RESOURCE	SOURCE	IDENTIFIER
Biotin anti-mouse CD115 (CSF-1R) Antibody	Biolegend	Cat # 135,507
CD102 (clone 3C4[mIC2/4])	ThermoFisher	Cat # 16-1021-82
LEAF™ Purified anti-mouse CD11a Antibody (clone M17/4)	Biolegend	Cat # 101,109
LEAF™ Purified anti-mouse CD54 Antibody (clone YN1/1.7.4)	Biolegend	Cat # 116,109
LEAF™ Purified Rat IgG2a, κ Isotype Ctrl Antibody (clone RTK2758)	Biolegend	Cat # 400,516
LEAF™ Purified Rat IgG2b, κ Isotype Ctrl Antibody (clone RTK4530)	Biolegend	Cat # 400,622
LEAF™ Purified anti-mouse IFNAR-1 Antibody (clone MAR1-5A3)	Biolegend	Cat # 127,303
Ultra-LEAF™ Purified Mouse IgG1a, κ Isotype Ctrl Antibody (clone MOPC-21)	Biolegend	Cat # 400,165
Bacterial and virus strains		
MLV co-packaged with MLV LTR-GFP	Sewald lab	NA
MLV Gag-GFP	Sewald lab	NA
MLV CD63 LTR-GFP VLP	Sewald lab	NA
Chemicals, peptides, and recombinant proteins		
CellTrace FarRed dye	ThermoFisher	Cat #C34564
DYNAL™ Dynabeads™ Maus T-Aktivator CD3/CD28	Gibco	Cat # 11456D
MojoSort™ Streptavidin Nanobeads	Biolegend	Cat # 480,016
Paraformaldehyde (PFA)	Electron Microscopy Sciences	Cat # 15,710
Recombinant Mouse IL-15 (carrier-free)	BioLegend	Cat # 566,304
Recombinant Mouse IL-7 (carrier-free)	BioLegend	Cat # 577,804
Recombinant Mouse IL-4 (carrier-free)	BioLegend	Cat # 574,304
Recombinant Mouse IL-5 (carrier-free)	BioLegend	Cat # 581,504
Recombinant Mouse IL-6 (carrier-free)	BioLegend	Cat # 575,704
Recombinant Human TGF-β1 (carrier-free)	Biolegend	Cat # 580,704
Recombinant Human IL-2 (carrier-free)	Biolegend	Cat # 589,104
Retinoic acid	Sigma-Aldrich	Cat #R2625
LPS, ultrapure	Invivogen	Cat # tlrl-pb5lps
Ionomycin	Life technologies	Cat #I3909-1ML
phorbol 12-myristate 13-acetate (PMA)	Sigma Aldrich	Cat # 19-144
Ultra-LEAF™ Purified anti-mouse CD3ε Antibody (clone 145-2C11)	BioLegend	Cat # 100,340
Ultra-LEAF™ Purified anti-mouse CD28 Antibody (clone 37.51)	BioLegend	Cat # 102,116
Probenecid	Invitrogen	Cat #P36400
Fibronectin (solution, human)	Advanced BioMAtrix	Cat # 5050
Liberase TL	Roche	Cat # 5,401,020,001
DNase I	Roche	Cat # 4,716,728,001
Critical commercial assays		
Naive CD4$^+$ T cell isolation kit, mouse	Miltenyi Biotech	Cat # 130-104-453
BD Cytofix/Cytoperm™ kit	BD Biosciences	Cat # 554,714
LiveBLAzer™ FRET B/G Loading Kit	Invitrogen	Cat #K1095
Experimental models: Cell lines		
S49.1 T lymphoid cell line (ATCC, TIB-28)	ATCC	Cat # TIB-28
HEK293T	ATCC	Cat # CRL-1573
HEK293T-BlaM	Manuel Albanese (from Wolfgang Hammerschmidt lab)	Albanese et al., 2020
Experimental models: Organisms/strains		
C57BL/6J	Charles River	Strain Code: 632
B6.129S7-Itgaltm1Bll/J (CD11a−/−)	Jackson Laboratory	Stock No: 005,257

(*Continued on next page*)

Continued

REAGENT or RESOURCE	SOURCE	IDENTIFIER
B6.129S4-Icam1tm1Jcgr/J (ICAM1−/−)	Jackson Laboratory	Stock No: 002,867
Tg(CAG-DsRed*MST)1Nagy/J (RFP+)	Jackson Laboratory	Stock No: 006,051
Recombinant DNA		
pLRB303-FrMLV	Mothes Lab, Yale University	NA
pMMP-LTR-GFP	Mothes Lab, Yale University	NA
pLRB303-GagGFP	Mothes Lab, Yale University	Jin et al., 2009
MLV GagPol	Mothes Lab, Yale University	NA
pcDNA3-FrMLV Env	Mothes Lab, Yale University	NA
Software and algorithms		
FlowJo, V10	Treestar	NA
Graphpad Prism 9	GraphPad Software	NA
Photoshop CC	Adobe Systems	NA
Illustrator CC	Adobe Systems	NA
Other		
96-well transwell insert (3 μm pore size)	Corning	Cat # 3385
Cell strainer, 70 μm	Falcon	Cat # 352,350
5 mL Round Bottom Polystyrene Tube with Cell Strainer Snap Cap, 70 μm	Falcon	Cat # 352,235

RESOURCE AVAILABILITY

Lead contact

Further information and requests for resources and reagents should be directed to and will be fulfilled by the lead contact, Xaver Sewald (sewald@mvp.lmu.de).

Materials availability

This study did not generate new unique reagents.

Data and code availability

- All data reported in this paper will be shared by the lead contact upon request.
- This paper does not report original code.
- Any additional information required to reanalyze the data reported in this paper is available from the lead contact upon request.

EXPERIMENTAL MODEL AND SUBJECT DETAILS

Mice

C57BL/6 mice were obtained from Charles River. CD11a-deficient [B6.129S7-Itgaltm1Bll/J], ICAM1-deficient mice [B6.129S4-Icam1tm1Jcgr/J] and mice expressing cytoplasmic DsRed [Tg(CAG-DsRed*MST)1Nagy/J] (designated RFP + mice) in all nucleated cells were obtained from Jackson Laboratory. Six- to 12-week-old male and female mice were used for all experiments. No impact of sex nor age was observed on the reported phenotypes. Mice were maintained in groups of two to five under specific pathogen-free conditions at the Max von Pettenkofer-Institute. All mouse experiments were approved by the government of upper Bavaria and were performed in accordance to the legal requirements.

Cell lines and primary cell cultures

All cells were cultured under humified atmosphere at 37°C and 5% CO2. HEK293 cells (ATCC, CRL-1573) were cultured in RPMI-1640 medium supplemented with 10% heat-inactivated fetal calf serum (all from Life technologies). S49.1 cells (ATCC, TIB-28) were maintained in RPMI-1640 medium supplemented with 10% heat-inactivated fetal calf serum, 1% MEM non-essential amino acids, 10 mM sodium-pyruvate, 55 μM 2-mercaptoethanol (all from Life technologies) and 10 mM HEPES (Carl Roth). All cell lines were frequently tested to be mycoplasma negative.

All primary cells were isolated from 6-12 week-old male and female C57BL/6, CD11a-/-, ICAM1-/- mice and RFP + mice. Primary cells were cultured in RPMI-1640 medium supplemented with 10% heat-inactivated fetal calf serum, 1% MEM non-essential amino acids, 10 mM sodium-pyruvate, 55 μM 2-mercaptoethanol (all from Life technologies) and 10 mM HEPES (Carl Roth).

METHOD DETAILS

Primary cell isolation

B1 cells and primary macrophages were isolated from peritoneal cavity cells of C57BL/6, CD11a-/-, ICAM1-/- mice and RFP + mice by negative selection using biotinylated antibodies and subsequent magnetic separation with Streptavidin Nanobeads (Biolegend). For B1 cell enrichment, biotinylated antibodies against CD4, CD8, F4/80, Gr-1, TER-119, CD11c, NK1.1, CD23, CD88, CD117, CD115 and Fc-epsilon (all from Biolegend) were used. Macrophages were isolated using biotinylated antibodies against CD19, CD8, CD4, Gr-1, TER119 and CD11c (all from Biolegend). Both cell types were enriched to over 85% purity, as confirmed by flow cytometry. Naïve CD4+ T cells were isolated from splenocytes of C57BL/6, CD11a-/-, ICAM1-/- mice and RFP + mice using the naive CD4+ T cell isolation kit from Miltenyi Biotec.

Primary cell activation and differentiation *in vitro*

The following conditions were used for B1 cell and CD4+ T cell stimulation. Enriched B1 cells were activated using 2.5 μg/mL LPS (ultrapure, Invivogen) in the presence of mouse IL-4, mouse IL-5 and mouse IL-6 (each 100 ng/mL; Biolegend) for 24 h at 37°C. Naïve CD4+ T cells were activated with ionomycin (1 μM; Life technologies) and phorbol 12-myristate 13-acetate (PMA), (10 ng/mL; Sigma Aldrich) or by incubation with surface-bound antibodies against CD3ε and CD28 (Biolegend). For surface coating of 96-well plates, 100 μL antibody mix containing 1 μg of each antibody in PBS was used per well and incubated for 2-3 h at 37°C followed by a washing step with 200 μL PBS.

Naïve CD4+ T cells were differentiated into FoxP3-expressing T cells by cultivation in anti-CD3ε/CD28-coated 96-well plates in the presence of human IL-2 (20 ng/mL; Biolegend), mouse IL-7 (100 ng/mL; Biolegend), mouse IL-15 (100 ng/mL; Biolegend), human TGF-beta1 (5 ng/mL; Biolegend) and retinoic acid (10 nM; Sigma-Aldrich) at 37°C for at least 48 h. FoxP3-expression was confirmed by flow cytometry after intracellular staining using the BD Cytofix/Cytoperm Kit and anti-FoxP3 antibody (clone MF-14; Biolegend).

Virus preparation

Replication-competent reporter MLV was generated by co-transfecting HEK293 cells with pLRB303-FrMLV that encodes full-length replication competent Friend 57 ecotropic MLV, pMMP-LTR-GFP (encoding cytoplasmic GFP, ratio 10:1) and pLZRS-FrMLV Env to enhance the infectivity of the virus. Culture supernatants from HEK293 cells were harvested 24 and 48 h after co-transfection, filtered with nylon membrane filters (0.45 μm), aliquoted, and stored at −80°C. Viruses in supernatant were concentrated by sedimentation with a 15% sucrose/PBS cushion at 20,000 x g and 4°C for 2 h, and viral titers were determined by titrating concentrated virus on the murine S49.1 T lymphoid cell line (ATCC, TIB-28). GFP expression was determined after 24 h by flow cytometry on a BD FACSLyric.

In vitro trans-infection assay

Co-culture between target lymphocytes (B1 cells, activated CD4+ T cells, CD4+ FoxP3+ T cells) and donor macrophages was used to study *trans*-infection of MLV *in vitro*. B1 cells and CD4+ T cells were activated for 24 h with LPS and PMA/ionomycin, respectively, before co-culture. CD4+ FoxP3+ T cells were used for co-culture with macrophages 48 h after start of differentiation. Primary macrophages (donor cells) were seeded with a density of 2×10^5 cells per well in a 96-well plate and incubated for 24 h at 37°C to allow for CD169 surface expression. For co-culture, CD169 + macrophages were loaded with 1.5×10^5 infectious units (i.u.) of MLV LTR-GFP per well followed by incubation for 30 min at room temperature to allow virus surface binding. After incubation, unbound virus was removed by extensive washing with primary cell medium. Target cells were added to the macrophages in a 1:2 ratio and incubated at 37°C for 24 h. Infection of target cells was analyzed based on GFP expression by flow cytometry on a BD FACSLyric.

Antibody blocking of the adhesion proteins LFA1, ICAM1 (CD54) and ICAM2 (CD102) was performed by addition of antibodies (2 μg/well) against CD11a (clone M17/4, Biolegend), CD54 (clone YN1/1.7.4, Biolegend) and CD102 (clone 3C4[mIC2/4], ThermoFisher) during co-culture with MLV-laden macrophages for 24 h. IgG2a and IgG2b antibodies (2 μg/well; Biolegend) were used as isotype control.

For *trans*-infection assays with antibody blocking of CD169, CD169 + macrophages were incubated with 1.7 μg blocking antibodies against CD169 (clone 3D6.112, Biolegend) in primary cell medium for 20 min at RT. Macrophages were washed and incubated with concentrated MLV LTR-GFP reporter virus (1.5×10^5 i.u.) for 30 min at room temperature to allow virus binding. Unbound virus was removed by extensive washing with primary cell medium before co-culture with 1×10^5 target cells for 24 h.

For transwell co-cultures, 2×10^5 peritoneal cavity-derived macrophages were seeded in the 96-well transwell insert (3 μm pore size, Corning) and incubated for 24 h. Concentrated MLV LTR-GFP (2×10^5 i.u./well) was added to CD169 + macrophages and incubated for 30 min at RT to allow virus binding. Unbound virus was removed by extensive washing with primary cell medium. S49.1 target cells were added in the lower transwell compartment at a density of 2×10^5 cells in 200 μL. Transwell insert and lower transwell compartment were combined and incubated for 24 h at 37°C. Target cells were collected for fixation with 4% PFA, and infection was analyzed based on GFP expression by flow cytometry on a BD FACSLyric.

In vitro transduction of primary cells with MLV

Cells were transduced with MLV LTR-GFP by spin infection in a 96-well plate with flat bottom. Around 4×10^5 LPS-activated B1 cells or CD4+ FoxP3+ T cells were seeded per well and mixed with MLV LTR-GFP suspension (2×10^5 i.u./well). Spin infection was performed at 1,100 x g for 90 min at 37°C.

For *in vitro* transduction without spin infection, CD4+ FoxP3+ T cells (2×10^5 cells, differentiated for 48 h) were seeded in a 96-well plate and concentrated MLV LTR-GFP (2×10^5 i.u./well) was added to each well. After incubation for 24 h at 37°C, cells were fixed with 4% PFA and infection was analyzed based on GFP expression by flow cytometry on a BD FACSLyric.

In vitro cis-infection assay

Co-culture between target lymphocytes (CD4+ FoxP3+ T cells) and MLV-infected donor cells (B1 cells, CD4+ FoxP3+ T cells) was used to study *cis*-infection of MLV *in vitro*. Donor B1 and T cells were transduced with MLV LTR-GFP reporter virus by spin infection. After 24 h, remaining input virus was removed from donor cells by treatment with Trypsin/EDTA for 2 min at 37°C following one washing step with PBS/2 mM EDTA (all from Life technologies). Trypsin activity was inhibited by addition of primary cell culture medium, supplemented with 30% heat-inactivated fetal calf serum (Life technologies), and incubation at 4°C for 5 min.

Trypsinized donor B1 and T cells (1×10^5 each), respectively, were co-cultured in a flat-bottom 96-well plate at a ratio of 1:2 with CD4+ FoxP3+ T cells for 24 h at 37°C. Cells were cultured in primary cell culture medium in the presence of mouse IL-5, mouse IL-6, mouse IL-7 and mouse IL-15 (all 100 ng/mL; Biolegend).

Antibody blocking of the adhesion proteins LFA1 (CD11a/CD18 heterodimer) and ICAM1 (CD54) was performed by pre-treatment of CD4+ FoxP3+ target T cells with antibodies (2 μg/well) against CD11a (clone M17/4) and CD54 (clone YN1/1.7.4) (all from Biolegend) for 30 min at 37°C before addition of donor B1 cells for co-culture. IgG2a and IgG2b antibodies (2 μg/well; Biolegend) were used as isotype control.

For transwell co-cultures, 2×10^5 CD4+ FoxP3+ T cells were seeded in the fibronectin-coated (1 μg/well, Advanced BioMatrix) lower compartment of a 96-well transwell plate (Corning). 1×10^5 trypsinized donor B1 cells were added to the transwell insert (3 μm pore size) followed by incubation at 37°C for 24 h.

After 24 h of co-culture, MLV-infected target T cells were distinguished from donor B1 cells by immunostaining against CD19 (clone 1D3, Biolegend) and GFP expression was analyzed by flow cytometry on a BD FACSLyric. The ratio of GFP + target cells to GFP + donor cells was determined for each sample to quantify retrovirus spread.

CD169 expression by primary macrophages

To analyze if *in vitro* CD169 expression of peritoneal cavity-derived macrophages requires IFN type I signaling, freshly isolated macrophages were seeded with a density of 2×10^5 cells per well in a 96-well plate. Different amounts of blocking antibodies against IFNAR-1 or IgG1 isotype control antibodies (both from Biolegend) were added and cells were incubated for 24 h at 37°C. Macrophages were detached by incubation in PBS/2 mM EDTA for 10 min at 4°C and gentle pipetting. Cells were stained with antibodies against F4/80 and CD169 (both from Biolegend) before fixation with 4% PFA and flow cytometric analysis on a BD FACSLyric.

MLV Gag-GFP binding by CD169 + macrophages

To analyze CD169-dependent binding of MLV to peritoneal cavity-derived macrophages, cells were seeded with a density of 2×10^5 cells per well in a 96-well plate and incubated for 24 h at 37°C. CD169 + macrophages were incubated with 1.7 μg blocking antibodies against CD169 (clone 3D6.112; Biolegend) in primary cell medium for w at RT. Afterward macrophages were washed and incubated with concentrated MLV Gag-GFP (3×10^5 i.u.) for 30 min at room temperature to allow virus surface binding. Unbound virus was removed by extensive washing with primary cell medium and macrophages were incubated for another 15 min at 37°C. Subsequently, cells were detached by incubation for 10 min at 4°C in PBS/2 mM EDTA and by gentle pipetting. Macrophages were fixed with 4% PFA and MLV Gag-GFP binding was analyzed by flow cytometry on a BD FACSLyric.

In vitro transduction of macrophages with MLV VLPs

To test whether peritoneal cavity-derived macrophages are permissive for MLV infection *in vitro*, cells were seeded with a density of 2×10^5 cells per well in a 96-well plate and incubated for 24 h at 37°C to allow for CD169 expression. CD169 + macrophages were loaded with 2×10^5 i.u. per well of MLV VLPs containing the reporter genome LTR-GFP, pseudotyped with glycoproteins from ecotropic MLV (ecoEnv) or VSV (VSV-G). After 24 h of incubation at 37°C, macrophages were detached by incubation for 10 min at 4°C in PBS/2 mM EDTA and gentle pipetting. Macrophages were fixed with 4% PFA and infection was analyzed based on GFP expression by flow cytometry on a BD FACSLyric.

Retrovirus capture and infection *in vivo*

For *in vivo* infection and virus capture experiments MLV LTR-GFP and fluorescent MLV Gag-GFP, respectively, were concentrated by sedimentation through a 15% sucrose/PBS cushion. Concentrated virus suspension (20 μL, corresponding to 8×10^4 or 2×10^4 i.u.) was subcutaneously (s.c.) injected into the footpads of C57BL/6, CD11a-/- and ICAM1-/- mice. Draining popliteal lymph nodes (pLNs) were isolated 2 or 5 days (MLV LTR-GFP) and 1 h (MLV Gag-GFP) after virus injection and prepared for flow cytometry by

incubation with Liberase TL (0.2 mg/mL, Roche) and DNase I (20 μg/mL, Roche) for 20 - 30 min at 37°C. Enzymes were inactivated by addition of excess RPMI medium containing 10% FCS followed by passing the tissue through a 70 μm cell strainer. After washing cells once with PBS/1% BSA/0.5 mM EDTA total cell numbers were determined, and samples were stained with antibodies for flow cytometry analysis.

Flow cytometry

Single cells from lymph nodes were blocked at 4°C for 20 min in PBS/1% BSA containing 10% rat serum (Jackson ImmunoResearch) and Fc-blocking antibody against CD16/CD32 (clone 93, Biolegend) before staining with antibodies for flow cytometry analysis. The following antibodies were used in the study: CD169-PE (clone 3D6.112), CD169-AF647 (clone 3D6.112), CD11b-APC (clone M1/70), CD11b-BV421 (clone M1/70), CD11b-PE/Cy7 (clone M1/70), CD11a-APC (clone M17/4), CD11c-APC (clone N418), CD54-APC (clone YN1/1.7.4), CD3e-BV421 (clone 145-2C11), CD3-PE (clone 17A2), CD3e-PE/Cy7 (clone 145-2C11), CD4-APC/Fire750 (clone GK1.5), CD19-PE (clone 6D5), CD19-APC (clone 6D5), CD19-BV421 (clone 6D5), CD44-APC (clone IM7), CD44-BV605 (clone IM7), CD62L-BV421 (clone MEL-14), CD62L-PE/Cy7 (clone MEL-14), CD102-AF647 (clone 3C4[MIC2/4]), FoxP3-AF647 (clone MF-14), FoxP3-PE (clone MF-14) and F4/80-PE/Cy7 (clone BM8). All antibodies were obtained from Biolegend. For intracellular staining of FoxP3 samples were prepared according to the BD Cytofix/Cytoperm kit and analyzed by flow cytometry. Data were acquired on a BD FACSLyric flow cytometer (BD Biosciences) and were analyzed with FlowJo software (Version 10, Treestar). The number of independent replicates for each experiment is mentioned in the figure legends. Each dot represents a single popliteal lymph node sample.

Adoptive transfer experiments

T cell populations were sorted from pooled lymph nodes (popliteal, inguinal, iliac) of RFP + mice on a BD FACSAria Fusion after antibody staining of CD4, CD44 and CD62L. Sorted RFP + lymphocyte populations (150,000–500,000 cells) and naïve CD4+ T cells (5×10^5 cells), isolated from the spleen of RFP + mice by negative selection (Miltenyi Biotec), were adoptively transferred in C57BL/6 mice by s.c. injection into the hind hock. After 24 h, mice were infected with MLV LTR-GFP (8×10^4 i.u.) and infected RFP + T cells were analyzed 48 h post infection for GFP expression by flow cytometry on a BD FACSLyric.

In vivo cis-infection assay

To study *cis*-infection *in vivo*, naïve CD4+ T cells were purified from splenocytes of C57BL/6, CD11a-/- and ICAM1-/- mice using the naïve CD4+ T cell isolation kit (Miltenyi Biotec), followed by CD3/CD28-mediated activation and differentiation into CD4+ FoxP3+ T cells for 48 h. CD4+ FoxP3+ T cells were transduced *in vitro* with MLV reporter virus by spin infection. After 24 h, residual virus particles were removed from CD4+ FoxP3+ T cells by Trypsin/EDTA treatment for 2 min at 37°C (Life technologies). Trypsin activity was blocked by addition of primary cell culture medium supplemented with 30% fetal calf serum (Life technologies) and incubation for 5 min at 4°C. To differentiate between adoptively transferred donor cells and newly infected target cells, donor CD4+ FoxP3+ T cells were stained with 1 μM CellTrace FarRed dye (ThermoFisher) in Opti-MEM medium (Life technologies) at a concentration of 1×10^6 cells/mL for 20 min at 37°C. Unbound dye was adsorbed by adding 5x volume of primary cell medium to the cell suspension and incubation for 10 min at 37°C. Subsequently, 1×10^6 MLV-transduced, FarRed-positive CD4+ FoxP3+ T cells were adoptively transferred by s.c. hock injection into C57BL/6, CD11a-/- and ICAM1-/- mice. Around 60 h post injection, draining popliteal lymph nodes were isolated from euthanized mice and single cell suspensions were analyzed by flow cytometry for newly infected GFP-positive cells (APC- GFP+) and FarRed-positive donor cells (APC + GFP-, APC + GFP+). The ratio of APC-GFP + to APC + GFP + cell was determined for each sample as a quantification of retrovirus spread.

In vivo trans-infection and fusion assay

To study *trans*-infection and fusion *in vivo*, naïve CD4+ T cells were purified from splenocytes of C57BL/6, CD11a-/- and ICAM1-/- mice using the naïve CD4+ T cell isolation kit (Miltenyi Biotec), followed by CD3/CD28-mediated activation and differentiation into CD4+ FoxP3+ T cells. After differentiation for 3 days, CD4+ FoxP3+ T cells were stained with 1 μM CellTrace FarRed dye (ThermoFisher) in Opti-MEM medium (Life technologies) at a concentration of 1×10^6 cells/mL for 20 min at 37°C. Unbound dye was removed by adding 5x volume of primary cell medium to the cell suspension and incubation for 10 min at 37°C.

Subsequently, 1×10^6 Far Red-positive CD4+ FoxP3+ T cells were adoptively transferred by s.c. injection into the hind hock of C57BL/6, CD11a-/- and ICAM1-/- mice. After 24 h, mice were infected by s.c. injection of MLV LTR-GFP or MLV VLPs containing CD63-BlaM (1.5×10^5 i.u.) into the footpad. Draining pLNs were isolated 2 h post injection of VLPs or 40 h post infection with MLV LTR-GFP to study fusion and *trans*-infection, respectively. After preparation of single cell suspensions, samples were analyzed by flow cytometry for fused cells or newly infected GFP-positive cells (APC- GFP+) and FarRed-positive donor cells (APC + GFP-, APC + GFP+). The ratio of APC + GFP+ (infection) or APC-CCF4cleaved (fusion) to total APC + cells was determined for each sample to quantify retrovirus *trans*-infection and *trans*-fusion efficiency, respectively.

In vitro and *in vivo* fusion assay

To detect fusion of virus particles with primary cells *in vitro*, virus like particles (VLPs) were produced in HEK293T cells that stably overexpress a codon-optimized β-lactamase enzyme (BlaM) fused to the carboxy-terminus of the tetraspanin CD63 (CD63-BlaM)

(Albanese et al., 2020). MLV VLPs incorporate CD63-BlaM into the envelope upon budding. VLPs containing the reporter genome LTR-GFP, pseudotyped with ecotropic MLV glycoprotein (ecoEnv) or VSV-G or VLPs lacking glycoprotein (ΔEnv), were concentrated by sedimentation through a 15% sucrose/PBS cushion.

To quantify fusion of VLPs with cells *in vitro*, 2×10^5 cells (primary CD4+ T cells, S49.1 cells, CD169 + macrophages) per well of a 96-well plate were incubated for 4 h with 2×10^5 i.u. of concentrated CD64-BlaM VLPs (directly or via *trans*-infection with VLPs bound to CD169 + primary macrophages). After incubation, cells were washed with CO2-independent medium/10% FCS to remove unbound virus. Subsequently, 100 μL staining solution was added to the cells. Incubation with staining solution comprising of CO2-independent medium/10% FCS supplemented with 2.5 mM probenecid (Invitrogen) and 2 μL/mL CCF4-AM substrate as well as 8 μL/mL Solution B (both from LiveBLAzer™ FRET B/G Loading Kit, Invitrogen) was performed over night at room temperature to allow cytoplasmic uptake and enzymatic cleavage of the CCF4-AM substrate. Subsequently, samples were washed 2 x with PBS/1% BSA and fixed with 4% PFA. Fusion of CD63-BlaM VLPs with a cell results in cytoplasmic localization of BlaM and subsequent CCF4 substrate cleavage. Cleaved substrate can be quantified using flow cytometry by a shifted emission wavelength from 520 nm of the uncleaved substrate to 447 nm in the case of cleaved CCF4.

To quantify retrovirus fusion *in vivo* at pLNs, concentrated CD64-BlaM VLPs (2×10^5 i.u.) were s.c. injected into the footpad of C57BL/6 mice. At different time points post injection, mice were sacrificed and draining pLNs were isolated for preparation of single cell suspensions. Total cell numbers of pLNs were determined and samples were processed as described above for flow cytometric analysis. To characterize VLP-fused cell types, antibodies against cell type-specific surface markers were used as described above.

QUANTIFICATION AND STATISTICAL ANALYSIS

Statistical comparisons were performed using GraphPad Prism 9 software under the assumption that the samples did not follow a Gaussian distribution. For two-group comparisons, the non-parametric Mann-Whitney test (two-tailed) was used. Exact p values and the numbers of independent replicates (n) are mentioned in the figures or figure legends. A difference was interpreted as statistically significant if $p < 0.05$.